TIME- OR FREQUENCY-DOMAIN EQUALIZATION FOR WIDEBAND OFDM CHANNELS?

Tao Xu[*]*, Zijian Tang*[♭]*, Geert Leus*[*]*, and Urbashi Mitra*[†]

[*] Fac. EEMCS, Delft University of Technology, Mekelweg 4, 2628CD, Delft, Netherlands

[♭] TNO, Oude Waalsdorperweg 63, 2597 AK The Hague, Netherlands

[†] Ming Hsieh Department of Electrical Engineering, University of Southern California, Los Angeles, USA

ABSTRACT

OFDM suffers from inter-carrier interferences in the presence of the time variation. This paper seeks to quantify the amount of interferences resulting from wideband channels which assumed to follow the multi-scale/multi-lag (MSML) model. Due to the fact that the mobility in wideband channels induces scale effects, Doppler is revealed in a manner distinct from the frequency shifts experienced in narrowband systems. The MSML channel model results in full channel matrices both in the frequency and time domains. However, banded approximations are still possible, leading to significant reduction in the equalization complexity. Herein, measures for determining whether time-domain or frequency-domain should be undertaken are provided based on the amount of the resulting interference.

Index Terms— Wideband channels, OFDM, equalization,

1. INTRODUCTION

Wideband time-varying channels are of interest in a variety of wireless communication scenarios, e.g. ultrawideband terrestrial radio frequency systems or underwater acoustic systems. Due to the nature of wideband propagation, such channels exhibit fundamental differences with respect to so-called *narrowband* channels. In particular, it has been shown that multi-scale, multi-lag (MSML) channel descriptions offer improved modeling of wideband channels over multi-Doppler-shift, multi-lag models [1]. Orthogonal frequency-division multiplexing (OFDM), as a typical frequency-domain (FD) transmission, is still attractive to be employed in wideband channels. Approaches include splitting the wideband channel into parallel narrowband channels [2] or assuming a simplified model which reduces the wideband channel to a narrowband channel subject a carrier frequency offset (CFO) [3]. However, prior works ignore the MSML nature of wideband channels. The FD equalization of block transmissions over MSML channels is considered in [4]. However, a quantitative analysis of the inter-carrier interference (ICI) of OFDM over such MSML channels is still lacking.

In narrowband systems, it is well-known that we can equalize the time-varying channel either in the time domain (TD) or in the in the frequency domain [5]. The choice is determined by which domain leads to a less equalization complexity than the other domain to achieve the same performance. This paper is to research the same question but in wideband systems, and argue that it is sometimes attractive to perform equalization in the time-domain instead of the classical frequency domain approaches employed for OFDM. We begin with a detailed interference analysis of the Doppler effect on wideband channels both in the frequency domain and time domain. In particular, we show that the channel matrices in both domains are

full matrices when subject to Doppler. However, the distribution of the interference energy is governed by a different mechanism in the frequency domain than in the time domain. Based on this observation, we derive a proper approximation method for the corresponding channel matrices to reduce the equalization complexity. A concise metric is proposed as a criterion for determining in which domain the equalization is more appealing.

Notation: Upper (lower) bold-face letters stand for matrices (vectors); superscript H denotes Hermitian; we reserve j for the imaginary unit, $<k>$ for integer rounding of a number k, $[\mathbf{A}]_{k,m}$ for the (k,m)th entry of the matrix $\mathbf{A}$; $\mathrm{diag}(\mathbf{x})$ for a diagonal matrix with $\mathbf{x}$ on its main diagonal, and $\odot$ for the Hadamard product of two matrices.

2. SYSTEM MODEL BASED ON AN MSML CHANNEL

We consider a wideband time-varying channel, which is assumed to have L discrete paths. The lth path is characterized by the following three parameters: h_l, the path gain; u_l, the radial velocity which is uniquely determined by the incident angle of this path; and τ_l, the delay due to the traveling time. Suppose $x(t) = s(t)e^{j2\pi f_c t}$ denotes the transmit signal in the passband with a center frequency f_c. In compliance with the wideband channel assumption, the received signal resulting from the lth path $r_l(t)$ is related to $x(t)$ by $r_l(t) = h_l\sqrt{\alpha_l}x(\alpha_l(t-\tau_l))$, where $\alpha_l \approx 1 + \frac{2u_l}{c}$ is the scaling factor with c the speed of the communication medium.

With a collection of L paths, the input-output (I/O) relationship after down converting by $e^{-j2\pi f_c t}$ can be written as

$$r(t) = \sum_{l=0}^{L-1} h_l\sqrt{\alpha_l}s(\alpha_l(t-\tau_l))e^{j2\pi(\alpha_l-1)f_c t} + w(t), \quad (1)$$

where $w(t)$ stands for the baseband noise. We denote the channel embedded in (1) as a MSML channel if there exist at least two paths l and l', for which $\alpha_l \neq \alpha_l'$ and $\tau_l \neq \tau_l'$.

2.1. Frequency-Domain Channel Equalization

Suppose that the baseband transmit signal $s(t)$ consists of K subcarriers, and that onto each of the subcarriers, a data symbol b_k is modulated. As a result, we have

$$s(t) = \frac{1}{\sqrt{K}} \sum_{k \in \{0,1,\cdots K-1\}} b_k e^{j2\pi k \Delta f t}, \quad -T_{\mathrm{pre}} < t \leq KT \quad (2)$$

where T denotes the inverse of the signal bandwidth, and $\Delta f = 1/(KT)$. T_{pre} stands for the duration of the cyclic prefix (CP), which is assumed to be shorter than KT but larger than $\max_l(\alpha_l\tau_l)$ to avoid inter-block interference (IBI).

The receiver is assumed to be perfectly synchronized, and we want to sample the received signal $r(t)$ from the point where the CP

is stripped off. Due to the MSML channel assumption, the sampling rate at the receiver is not straightforwardly defined. Optimal resampling for MSML channels is discussed in [6]. For the moment, let us just assume that the receiver adopts a sampling rate of T/β with β being a positive number between $\min_l(\alpha_l)$ and $\max_l(\alpha_l)$ to represent the resampling ratio. Accordingly, we denote the nth received sample as $r_n^{(\beta)} = r(nT/\beta)$. Substituting (2) into (1), we have

$$r_n^{(\beta)} = \sum_{l=0}^{L-1} e^{j2\pi f_c \frac{\alpha_l-1}{\beta} nT} h_l^{(\beta)} \sum_{k=0}^{K-1} b_k e^{j2\pi \frac{\alpha_l}{\beta} \frac{kn}{K}} e^{-j2\pi \frac{\alpha_l \tau_l}{T} \frac{k}{K}} + w_n^{(\beta)},$$ (3)

where $w_n^{(\beta)} = w(nT/\beta)$, and $h_l^{(\beta)} = h_l \sqrt{\frac{\alpha_l}{\beta}} e^{-j2\pi \alpha_l \tau_l f_c}$.

Stacking $r_n^{(\beta)}$ for $n = [0, \cdots, K-1]$ into a vector $\mathbf{r}_T^{(\beta)} = [r_0^{(\beta)}, \cdots, r_{K-1}^{(\beta)}]^T$, we attain

$$\mathbf{r}_T^{(\beta)} = \sum_{l=0}^{L-1} h_l^{(\beta)} \mathbf{D}_l^{(\beta)} \mathbf{F}_{\alpha_l/\beta}^H \mathbf{\Lambda}_l \mathbf{b} + \mathbf{w}_T^{(\beta)},$$ (4)

$$= \underbrace{\left[\sum_{l=0}^{L-1} h_l^{(\beta)} \mathbf{D}_l^{(\beta)} \mathbf{F}_{\alpha_l/\beta}^H \mathbf{\Lambda}_l \mathbf{F}_1 \right]}_{\mathbf{H}_T^{(\beta)}} \mathbf{s} + \mathbf{w}_T^{(\beta)},$$ (5)

where $\mathbf{F}_\alpha$ represents a fractional discrete Fourier transform (DFT) matrix, whose (m,k)th entry can be expressed as

$$[\mathbf{F}_\alpha]_{m,k} = \frac{1}{\sqrt{K}} e^{-j2\pi\alpha \frac{mk}{K}}.$$ (6)

Obviously, $\mathbf{F}_1$ reduces to a normal DFT matrix; Further in (5), $\mathbf{b} = [b_0, \cdots, b_{K-1}]^T$ and $\mathbf{s} = [s_0, \cdots, s_{K-1}]^T$, which are related to each other by $\mathbf{b} = \mathbf{F}_1 \mathbf{s}$. In addition,

$$\mathbf{\Lambda}_l = \sqrt{K} \text{diag}(1, e^{j2\pi\alpha_l\lambda_l \frac{1}{K}}, \cdots, e^{j2\pi\alpha_l\lambda_l \frac{K-1}{K}}),$$ (7)

with $\lambda_l = \frac{\tau_l}{T}$ being the normalized delay of the lth path, and

$$\mathbf{D}_l^{(\beta)} = \text{diag}(1, e^{j2\pi\omega \frac{\alpha_l-1}{\beta} \frac{1}{K}}, \cdots, e^{j2\pi\omega \frac{\alpha_l-1}{\beta} \frac{K-1}{K}}),$$ (8)

with $\omega = \frac{f_c}{\Delta f}$ being the normalized frequency. Finally, $\mathbf{w}_T^{(\beta)}$ is similarly defined as $\mathbf{r}_T^{(\beta)}$.

In most of the cases, OFDM channels are equalized in the frequency domain. To this end, the received samples are first transformed into the frequency domain, resulting in

$$\mathbf{r}_F^{(\beta)} = \mathbf{F}_1 \mathbf{r}_T^{(\beta)} = \mathbf{H}_F^{(\beta)} \mathbf{b} + \mathbf{w}_F^{(\beta)},$$ (9)

with $\mathbf{w}_F^{(\beta)} = \mathbf{F}_1 \mathbf{w}_T^{(\beta)}$; $\mathbf{H}_F^{(\beta)}$ denotes the FD channel matrix

$$\mathbf{H}_F^{(\beta)} = \sum_{l=0}^{L-1} h_l^{(\beta)} \mathbf{H}_{F,l}^{(\beta)} \mathbf{\Lambda}_l^{(\beta)}$$ (10)

with $\mathbf{H}_{F,l}^{(\beta)} = \mathbf{F}_1 \mathbf{D}_l^{(\beta)} \mathbf{F}_{\alpha_l/\beta}^H$ being its lth component, whose (m,k)th entry is specified as

$$\begin{aligned}\left[\mathbf{H}_{F,l}^{(\beta)}\right]_{m,k} &= \sum_{n=0}^{K-1} e^{-j2\pi \frac{mn}{K}} e^{j2\pi\omega \frac{\alpha_l-1}{\beta} \frac{n}{K}} e^{j2\pi \frac{\alpha_l}{\beta} \frac{nk}{K}} \\ &= K e^{j \frac{(K-1)\pi}{K}\left((m-k)-(\xi_{l,F1}k+\xi_{l,F2})\right)} \times \\ &\quad \frac{\text{sinc}(\pi\left((m-k)-(\xi_{l,F1}k+\xi_{l,F2})\right))}{\text{sinc}(\frac{\pi}{K}\left((m-k)-(\xi_{l,F1}k+\xi_{l,F2})\right))},\end{aligned}$$ (11)

where $\xi_{l,F1} = \frac{\alpha_l-\beta}{\beta}$ and $\xi_{l,F2} = \frac{\alpha_l-1}{\beta}\omega$.

$\mathbf{H}_{F,l}^{(\beta)}$ is obviously a full matrix, with the non-zero off-diagonal entries representing the effect of ICI. In the absence of Doppler, we have $\alpha_l \equiv 1$ and thus $\beta = 1$. Then it follows that $\left[\mathbf{H}_{F,l}^{(\beta)}\right]_{m,k} =$

$\delta(m-k)$, and thus $\mathbf{H}_{F,l}^{(\beta)}$, as well as $\mathbf{H}_F^{(\beta)}$, becomes diagonal such that the system is free of ICI. In another special case where $\alpha_l \equiv \alpha$ for $l = 0, \cdots L - 1$, corresponding to a single-scale scenario assumed by many underwater communication works such as [3], the resampling ratio at the receiver should be $\beta = \alpha$, and the ICI then results from a carrier-frequency offset (CFO) determined by $\xi_{l,F2}$. However the ICI analysis for the MSML channels becomes more complicated, which we will discuss later on.

Frequency-domain equalization (FDE) can be readily applied on (9). For instance, a linear minimum mean square error (LMMSE) equalizer can be derived as

$$\hat{\mathbf{b}} = \left(\mathbf{H}_F^{(\beta)H} \mathbf{H}_F^{(\beta)} + \sigma^2 \mathbf{I}\right)^{-1} \mathbf{H}_F^{(\beta)H} \mathbf{r}_F^{(\beta)}.$$ (12)

In the above, we have assumed that the data symbols are i.i.d with a unit variance, and the noise is uncorrelated with the data, i.i.d with variance σ^2.

2.2. Time-Domain Channel Equalization

Just as a single-carrier channel can be equalized in the frequency domain, it is also possible to equalize an OFDM channel in the time domain. In (5), the TD channel matrix $\mathbf{H}_T^{(\beta)}$ is introduced. Similar to its FD counterpart, we can rewrite it as $\mathbf{H}_T^{(\beta)} = \sum_{l=0}^{L+1} h_l^{(\beta)} \mathbf{D}_l^{(\beta)} \mathbf{H}_{T,l}^{(\beta)}$ with $\mathbf{H}_{T,l}^{(\beta)} = \mathbf{F}_{\alpha_l/\beta}^H \mathbf{\Lambda}_l \mathbf{F}_1$ being its lth component, whose (m,k)th entry is given by

$$\begin{aligned}\left[\mathbf{H}_{T,l}^{(\beta)}\right]_{m,k} &= \sum_{n=0}^{K-1} e^{j2\pi \frac{\alpha_l}{\beta} \frac{mn}{K}} e^{j2\pi\alpha_l\lambda_l \frac{n}{K}} e^{-j2\pi \frac{nk}{K}} \\ &= K e^{j \frac{(K-1)\pi}{K}\left((k-m)-(\xi_{l,T1}m+\xi_{l,T2})\right)} \times \\ &\quad \frac{\text{sinc}(\pi\left((k-m)-(\xi_{l,T1}m+\xi_{l,T2})\right))}{\text{sinc}(\frac{\pi}{K}\left((k-m)-(\xi_{l,T1}m+\xi_{l,T2})\right))},\end{aligned}$$ (13)

where $\xi_{l,T1} = \frac{\alpha_l-\beta}{\beta}$ and $\xi_{l,T2} = \alpha_l\lambda_l$.

For time-domain equalization (TDE), the estimate of $\mathbf{s}$ is first obtained by means of an LMMSE equalizer

$$\hat{\mathbf{s}} = \left(\mathbf{H}_T^{(\beta)H} \mathbf{H}_T^{(\beta)} + \sigma^2 \mathbf{I}\right)^{-1} \mathbf{H}_T^{(\beta)H} \mathbf{r}_T^{(\beta)},$$ (14)

after which the data estimate is obtained as $\hat{\mathbf{b}} = \mathbf{F}_1^H \hat{\mathbf{s}}$.

3. TIME- OR FREQUENCY-DOMAIN EQUALIZATION?

As we see from the analysis above, both the FD and TD channel matrices are generally full, and hence their inversion admits a complexity that is cubic in the number of subcarriers. Recall that in narrowband OFDM systems, the FD channel matrix will also be full if the time-variation within one OFDM symbol cannot be neglected. To lower the equalization complexity in such cases, many works approximate the channel matrix to be strictly banded [7]. In wideband systems, we next provide an analysis on the out-of-band interference resulting from a banded approximation, which shall determine which domain leads to a less equalization complexity than the other domain to achieve the same performance.

3.1. Out-of-Band Interference Analysis

Let us begin with the FD channel matrix. It is insightful to first focus on the structure of its lth component $\mathbf{H}_{F,l}^{(\beta)}$. Although observed by other works e.g. [4], we quantitatively describe in (11) that most energy of the kth transmitted data symbol b_k is shifted via the lth path to the $\{k + \Delta_{F,l}(k)\}$th subcarrier with $\Delta_{F,l}(k) = < \xi_{l,F1}k + \xi_{l,F2} >$. It indicates that the frequency shift $\Delta_{F,l}(k)$ is

linearly dependent on the subcarrier index k through $\xi_{l,F1}$, with an offset $\xi_{l,F2}$. Different from narrowband time-varying systems where each subcarrier experiences a statistically identical Doppler shift, it is unique to wideband time-varying systems that the Doppler shift is linear to the subcarrier index.

The sinc function in (11) also suggests that the signal energy is mostly concentrated in subcarrier $k + \Delta_{F,l}(k)$ and its nearby subcarriers, and decays in subcarriers farther away. To appreciate how fast the signal energy decays, let us introduce $B_{F,l}(k)$ to quantify the number of subcarriers where most of the energy of b_k is located, which can thus be viewed as the bandwidth of $\mathbf{H}_{F,l}^{(\beta)}$ along its kth column. $B_{F,l}(k)$ is obtained by evaluating the following inequality

$$B_{F,l}(k) = \arg\min_B \sum_{m=k+\Delta_{F,l}(k)-B}^{k+\Delta_{F,l}(k)+B} \left| [\mathbf{H}_{F,l}^{(\beta)}]_{m,k} \right|^2 > \gamma \sum_{m=0}^{K-1} \left| [\mathbf{H}_{F,l}^{(\beta)}]_{m,k} \right|^2$$

$$\Rightarrow \arg\min_B \sum_{m=k+\Delta_{F,l}(k)-B}^{k+\Delta_{F,l}(k)+B} \left| \frac{\mathrm{sinc}(\pi\left((m-k)-(\xi_{l,F1}k+\xi_{l,F2})\right))}{\mathrm{sinc}(\frac{\pi}{K}\left((m-k)-(\xi_{l,F1}k+\xi_{l,F2})\right))} \right|^2$$

$$> \gamma \sum_{m=0}^{K-1} \left| \frac{\mathrm{sinc}(\pi\left((m-k)-(\xi_{l,F1}k+\xi_{l,F2})\right))}{\mathrm{sinc}(\frac{\pi}{K}\left((m-k)-(\xi_{l,F1}k+\xi_{l,F2})\right))} \right|^2, \quad (15)$$

where γ is a positive number no larger than 1. In Fig. 1, the relationship between $\max_k B_{F,l}(k)$ and γ is plotted, where it is clear that most of the signal energy of b_k is captured within a limited bandwidth. Notably, this bandwidth is almost independent of $\xi_{l,F1}$ and $\xi_{l,F2}$ as suggested by Fig. 1.

Since $\mathbf{H}_{F,l}^{(\beta)}$ is roughly banded, it is therefore reasonable to approximate $\mathbf{H}_F^{(\beta)}$, which is a weighted sum of $\mathbf{H}_{F,l}^{(\beta)}$, also as banded. As an example, we plot in Fig. 2 the structure of $\mathbf{H}_F^{(\beta)}$ where we assume that there are in total two paths. Obviously, the bandwidth of $\mathbf{H}_F^{(\beta)}$ at the kth column, denoted as $B_F(k)$, is

$$B_F(k) =$$
$$\max_l \left(k + \Delta_{F,l}(k) + B_{F,l}(k)\right) - \min_l \left(k + \Delta_{F,l}(k) - B_{F,l}(k)\right)$$
$$\approx \max_l \left(\Delta_{F,l}(k)\right) - \min_l \left(\Delta_{F,l}(k)\right) + 2\max_l \left(B_{F,l}(k)\right),$$

We refer the reader to Fig. 2 for the physical meaning of the notations. It is important to underscore that since the bandwidth $B_F(k)$ is dependent on the subcarrier index k, the boundaries of the band are not parallel to each other as in banding approaches for narrowband cases. With the band approximation, the equalizer will not employ $\mathbf{H}_F^{(\beta)}$, but the banded version $\tilde{\mathbf{H}}_F^{(\beta)} = \mathbf{P}_F \odot \mathbf{H}_F^{(\beta)}$, where the (m,k)th entry of $\mathbf{P}_F$ is equal to 1 if $\min_l (k + \Delta_{F,l}(k) - B_{F,l}(k)) \le m \le \max_l (k + \Delta_{F,l}(k) + B_{F,l}(k))$ or 0 otherwise. Such an equalizer experiences a signal-to-interference ratio (SIR) given by

$$\mathrm{SIR} = \frac{\|\tilde{\mathbf{H}}_F^{(\beta)}\|^2}{\|\mathbf{H}_F^{(\beta)} - \tilde{\mathbf{H}}_F^{(\beta)}\|^2}. \quad (16)$$

The above analysis can also be applied to the TD channel matrix $\mathbf{H}_F^{(\beta)}$ in an analogous manner. The bandwidth of $\mathbf{H}_F^{(\beta)}$ is defined vertically, related with the span of the row index, m, in (15), while the bandwidth of $\mathbf{H}_T^{(\beta)}$ will be defined horizontally, related with the span of the column index, k. We illustrate them in Fig. 3. More specifically, we define $\Delta_{T,l}(m) = <\xi_{l,T1}m + \xi_{l,T2}>$, and introduce $B_{T,l}(m)$ similarly as $B_{F,l}(k)$ is introduced in (15). Finally, the bandwidth of $\mathbf{H}_T^{(\beta)}$ at the mth row, denoted as $B_T(m)$, is given by $B_T(m) = \max_l (\Delta_{T,l}(m)) - \min_l (\Delta_{T,l}(m)) + 2\max_l (B_{T,l}(m))$, based on which we are able to obtain a banded approximation of $\mathbf{H}_T^{(\beta)}$ as $\tilde{\mathbf{H}}_T^{(\beta)} = \mathbf{P}_T \odot \mathbf{H}_T^{(\beta)}$ with $\mathbf{P}_T$ similarly defined as $\mathbf{P}_F$.
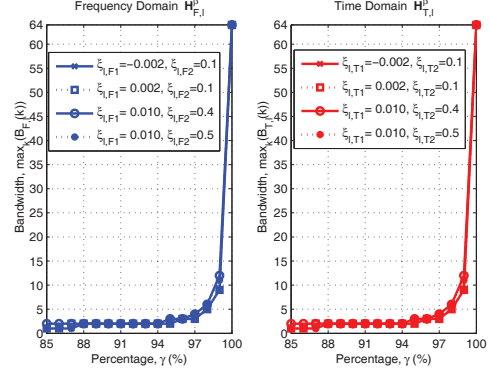

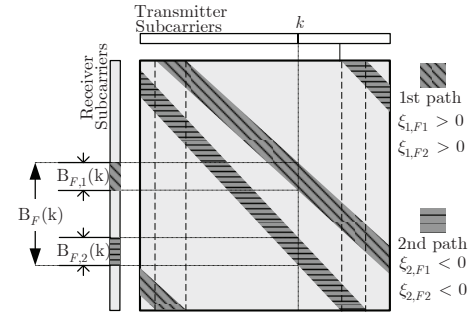**Fig. 1**. Bandwidth of $\mathbf{H}_{F,l}^{(\beta)}$ or $\mathbf{H}_{T,l}^{(\beta)}$

Fig. 2. Illustration of $\mathbf{H}_F^{(\beta)}$ correlated with paths

3.2. Criterion to choose FDE or TDE

With the LMMSE equalizer given in (12), it is clear that the cost of equalization in the frequency domain will be upper-bounded by $\mathcal{O}(KB_F^2)$ with $B_F = \max_k B_F(k)$. Likewise, the cost of equalization in the time domain will be upper-bounded by $\mathcal{O}(KB_T^2)$ with $B_T = \max_m B_T(m)$. To minimize the complexity, we use therefore the ratio B_F/B_T as the criterion to choose in which domain the equalization will be realized. However, the evaluation of B_F and B_T is a bit cumbersome, and lacks the insight of the channel physics. In practice, it is reasonable to assume that $\max_{l,k} (B_{F,l}(k)) \approx \max_{l,m} (B_{T,l}(m)) = C$ [see Fig. 1], and consequently, we consider the proportion

$$\epsilon = \frac{B_F - 2C}{B_T - 2C} = \frac{\max_k \left(\max_l(\Delta_{F,l}(k)) - \min_l(\Delta_{F,l}(k)) \right)}{\max_m \left(\max_l(\Delta_{T,l}(m)) - \min_l(\Delta_{T,l}(m)) \right)}.$$

For a realistic scale α_l, we are usually allowed to assume that

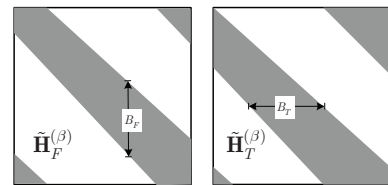$$\frac{|\alpha_l - \beta|}{\beta} \ll \frac{1}{K-1}, \quad (17)$$

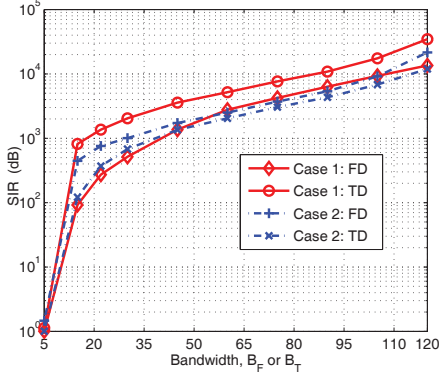**Fig. 3**. Structure of Approximated Matrix for FD and TD Channel

Fig. 4. SIR vs. B_F (B_T)

Fig. 5. BER vs. SNR for two cases

from which it follows that $\max_{l,k}(|\xi_{l,F1}|k) \ll 1$ and $\max_{l,m}(|\xi_{l,T1}|m) \ll 1$. With these assumptions, ϵ can further be rewritten as

$$\epsilon = \frac{\left\langle (\max_l(\alpha_l)-1)\frac{\omega}{\beta} \right\rangle - \left\langle (\min_l(\alpha_l)-1)\frac{\omega}{\beta} \right\rangle}{\left\langle \max_l(\alpha_l\lambda_l) \right\rangle - \left\langle \min_l(\alpha_l\lambda_l) \right\rangle}, \quad (18)$$

where $\omega = \frac{f_c}{\Delta f}$ is introduced in (8) as the normalized frequency, and $\lambda_l = \frac{\tau_l}{T}$ is introduced in (7) as the normalized delay of the lth path. (18) suggests that if the maximum difference between the Doppler shifts of each path (i.e., $\frac{\alpha_l - 1}{\beta}\omega$) is smaller than the maximum difference between the time shifts of each path (i.e., $\alpha_l\lambda_l$), then the equalization should be realized in the frequency domain, otherwise, a time-domain approach will be more appealing in terms of the complexity. Although a similar conclusion has been made for narrowband systems [5], its extension to wideband systems is not straightforward as shown above.

4. COMPUTER SIMULATIONS AND DISCUSSIONS

We consider two different types of wideband channels: 1) ultrawideband (UWB) radio channels, and 2) underwater acoustic channels (UAC). The channel parameters for these two cases are summarized in Table 1, except the path gain h_l, which is modeled in the simulation as a zero-mean i.i.d. variable whose variance σ_l^2 equals $c \cdot e^{|\lambda_l|}$ with c being a normalization constant such that $\sum_l \sigma_l^2 = 1$.

Table 1. Channel parameters

Case 1: $\epsilon > 1$			Case 2: $\epsilon < 1$		
$K = 128, \omega = 10000, \beta = 1$			$K = 128, \omega = 400, \beta = 1$		
l	α_l	λ_l	l	α_l	λ_l
0	1.0000	0.00	0	1.0000	0.00
1	1.0011	1.02	1	1.0011	5.02
2	1.0014	2.00	2	1.0014	7.00
3	0.9989	3.01	3	0.9989	10.01

We first evaluate (16) and plot the curve of the SIR versus B_F (B_T) in Fig. 4. It can be seen that for the same SIR, it is cheaper to equalize the UWB channel in the time domain where the Doppler spread is typically larger than the delay spread. In comparison, it is cheaper to equalize the UAC channel in the frequency domain since the UAC channel has usually a very long delay spread.

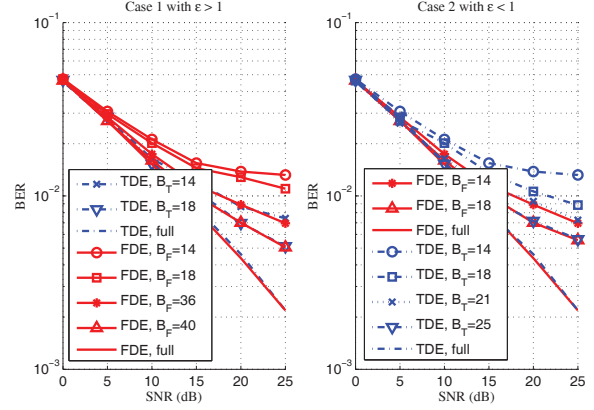Next, we compare the equalization performance. QPSK symbols are transmitted. The receiver, which is assumed to have perfect channel knowledge, utilizes the LMMSE equalizers given in (12) and (14). Note that for comparison, we use the banded approximation $\tilde{\mathbf{H}}_F^{(\beta)}$ ($\tilde{\mathbf{H}}_T^{(\beta)}$) in the equalizer for different bandwidths.

The left subplot of Fig. 5 plots the bit error rate (BER) performance as a function of signal-to-noise ratio (SNR) for the UWB channel in Case 1. It can be seen that the TD equalizer is computationally more attractive than the FD equalizer. For instance, the performance of the TD equalizer based on $\tilde{\mathbf{H}}_T^{(\beta)}$ with a bandwidth $B_T = 18$ achieves a similar BER as the FD equalizer based on $\tilde{\mathbf{H}}_F^{(\beta)}$ with a bandwidth $B_F = 40$. The BER performance for the UAC channel in Case 2 is compared in the right subplot of Fig. 5, where it is evident that the FD equalizer is more appealing in this case. These facts align with the observations made in Fig. 4.

5. CONCLUSIONS

Equalization of wideband channels in OFDM is discussed, where we use a multi-scale, multi-lag channel model. The resulting time-domain and frequency-domain channel matrices are shown to be approximately banded. We propose a criterion to determine in which domain the channel matrix is more banded than the other domain. This property is utilized to minimize the equalization complexity.

6. REFERENCES

[1] Y. Jiang and A. Papandreou-Suppappola. Discrete time-scale characterization of wideband time-varying systems. *IEEE T. Signal. Proces.*, 54(4):1364–1375, 2006.

[2] G. Leus and P. van Walree. Multiband OFDM for covert acoustic communications. *IEEE J. Sel. Area. Comm.*, 26(9):1662–1673, 2008.

[3] B. Li, S. Zhou, M. Stojanovic, L. Freitag, and P. Willett. Multicarrier communication over underwater acoustic channels with nonuniform doppler shifts. *IEEE J. Oceanic. Eng.*, 33(2):198–209, 2008.

[4] U. Mitra and G. Leus. Equalizers for multi-scale/multi-lag wireless channels. In *Proc. IEEE GLOBECOM'10*, pages 1–5, 2010.

[5] D. Falconer, S. L. Ariyavisitakul, A. Benyamin-Seeyar, and B. Eidson. Frequency domain equalization for single-carrier broadband wireless systems. *IEEE Commun. Mag.*, 40(4):58–66, 2002.

[6] S. Yerramalli and U. Mitra. Optimal resampling of OFDM signals for multiscale–multilag underwater acoustic channels. *IEEE J Oceanic Eng*, 36(1):126–138, 2011.

[7] L. Rugini, P. Banelli, and G. Leus. Simple equalization of time-varying channels for OFDM. *IEEE Commun. Lett.*, 9(7):619–621, 2005.